NBTI from the perspective of defect states with widely distributed time scales

B. Kaczer, T. Grasser[1], J. Martin-Martinez[2], E. Simoen, M. Aoulaiche, Ph. J. Roussel, G. Groeseneken[3]
IMEC, Kapeldreef 75, B-3001 Leuven, Belgium
[1] TU Wien, Austria
[2] UAB Barcelona, Spain
[3] also ESAT, KU Leuven, Belgium
phone: +32 (16) 281-557, fax: +32 (16) 281-706, e-mail: Ben.Kaczer@imec.be

***Abstract*—Broad similarity between negative bias temperature instability (NBTI) relaxation and 1/f noise is observed. Individual transitions in NBTI relaxation in small pFETs are observed and Poisson defect number statistics is inferred. Finally, it is argued that the wide distribution of defect times should be considered in addition to defect number variation in small devices.**

Keywords- pFET, reliability, negative bias temperature instability (NBTI), 1/f noise, single charge events

I. INTRODUCTION

Bias-temperature instabilities (BTI) in CMOS technologies with both conventional and advanced gate stacks remain at the forefront of reliability concerns. Central to the negative BTI (NBTI) mechanism is the existence of *defect states with a wide distribution of time scales*. This concept, constituting the chief complication for the proper evaluation and hence understanding of NBTI, is further developed here.

We first note that the very wide time scale distribution of defect states, observable e.g. in NBTI relaxation experiments, is also standardly invoked to explain the so-called 1/f noise spectra [1], observed in our devices. We further observe many other similarities in the properties of the NBTI relaxation component [2] and the FET noise spectrum, be it nitrogen concentration, temperature, voltage, or NBTI-stress dependences. This leads us to speculate that both are in fact due to the same (gate oxide) defects.

We further visualize the picture of discrete states by monitoring *individual* transitions in NBTI relaxation in small pFETs, allowing us to directly link the threshold voltage shift ΔV_{th} with the *number* of charged defects. Poisson defect number statistics is demonstrated.

Finally, we discuss the effect of the widely distributed time scales on the NBTI measurements and the switching of a digital inverter. We illustrate this by showing that defects with time scales visible in standard NBTI measurements could differ substantially from those active during inverter switching. We conclude that the distribution of defect *times* should be considered in addition to defect *number* variation in small devices and show how certain applications, such as SRAM, could be adversely affected.

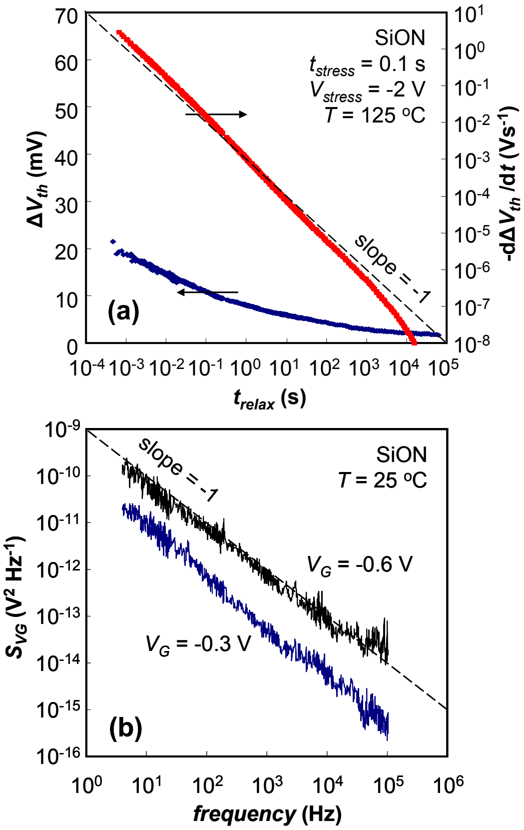

Figure 1. (a) Characteristic long, log-like ΔV_{th} relaxation tail is observed after even short (pulse-like) NBTI stress. The *rate* of recovery $d\Delta V_{th}/dt_{relax}$ following $1/t_{relax}$ for ~ 7 decades is a signature of states with discharging time constants covering as many decades. (b) Gate-referred noise spectra measured on the same (unstressed) devices show clear 1/f dependence, routinely explained by a superposition of states with widely distributed time scales [1].

II. EXPERIMENTAL

pFET devices with 1.4 nm EOT SiON / poly-Si gates [2] were used in most measurements. Where noted, pFETs with 2.0 – 2.4 nm CET HfSiO gate oxides and TaN gates were used, without or with NH_3 or DPN nitridation [3]. Extended measure-stress-measure (eMSM) technique was employed, alternating gate voltage V_G between V_{stress} and V_{meas} (chosen ≈ V_{th}) [2] at temperature $T = 125\ ^{o}C$ on 10 µm wide and 0.25 – 0.5 µm long devices and analyzed following Ref. [4]. NBTI fluctuations were monitored on $0.25 \times 0.25\ \mu m^2$ SiON pFETs. Noise measurements were performed on a dedicated setup at low $|V_G|$ to avoid stressing the tested device. NBTI stressing between noise measurements (Figure 5) was achieved by performing noise measurements at $V_G = V_{stress}$.

III. RESULTS AND DISCUSSION

A. *Similarities between NBTI relaxation and 1/f noise*

Long, log(t)-like behavior of ΔV_{th} is typically observed in both the initial portion of NBTI degradation [5, 6] and the recovery phase. Figure 1a illustrates that the *rate of degradation* $d\Delta V_{th}/dt_{relax}$ [7] extracted from the log(t_{relax})-like ΔV_{th} relaxation transient after even a *very short*, 0.1 s stress, follows $1/t_{relax}$ for over 7 decades. Such behavior is a signature of states with discharging time constants covering as many decades [2].

Incidentally, *superposition of relaxation of states with widely distributed time scales* is the standard explanation of the 1/f noise spectra [1], which are clearly observed in our pFETs (Figure 1b). This obvious similarity leads us to argue the possibility that the same states with widely distributed time scales in fact play a fundamental role in both NBTI and noise measurements.

This direct correspondence of both phenomena is further supported by several additional observations:

- Nitridation of a (high-k) gate stack results in a substantial increase in both the log(t)-like relaxation component and the 1/f noise spectra, as documented in Figure 2 [8, 9].
- At low V_G, the temperature dependences of both the relaxation rate and the 1/f noise are weak (Figure 3) [10].
- The relaxation component is observed to increase as $(V_{stress}\text{-}V_{meas})^2$ (Figure 4) [2,5]. Similarly, S_{VG} dependence goes like $(V_G\ \text{-}V_{th})^2$ as seen in Figure 2b.
- The impact of NBTI stress on both the noise (Figure 5) and the relaxation component of ΔV_{th} (shown e.g. in Figure 6a of Ref. [2]) is relatively weak [11].

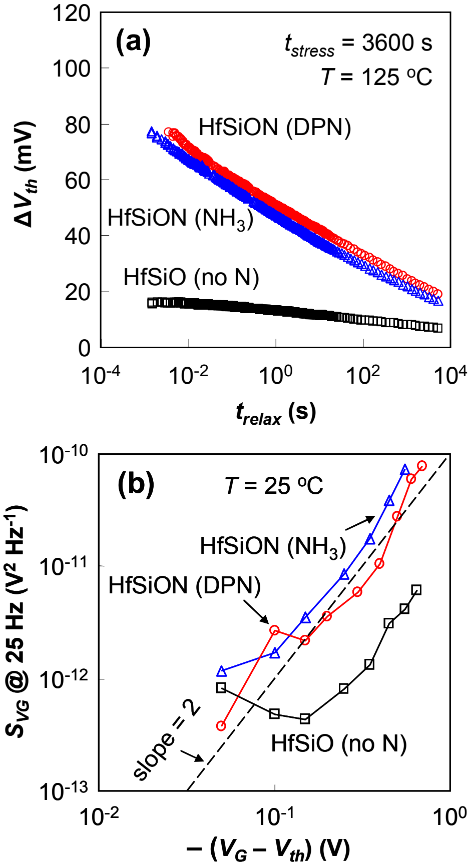

Figure 2. (a) Log-like relaxation component following stress at a fixed oxide electric field of ~ 9 $MVcm^{-1}$ is substantially larger in nitrided gate stacks [3]. (b) Similarly, nitrided stacks show much stronger noise S_{VG} than their non-nitrided counterpart. S_{VG} is observed approximately increasing with $(V_G\text{-}V_{th})^2$.

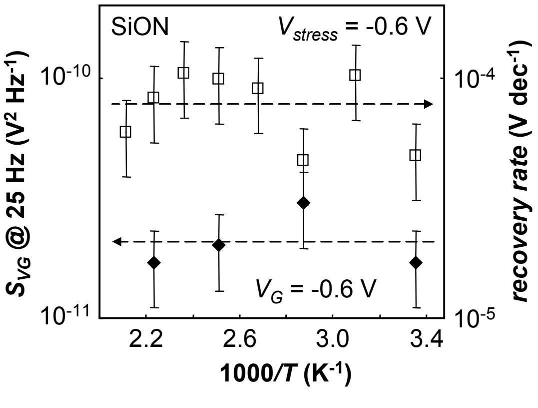

Figure 3. At low V_G, both the recoverable component rate [5] and noise spectrum S_{VG} have at most very weak temperature dependence.

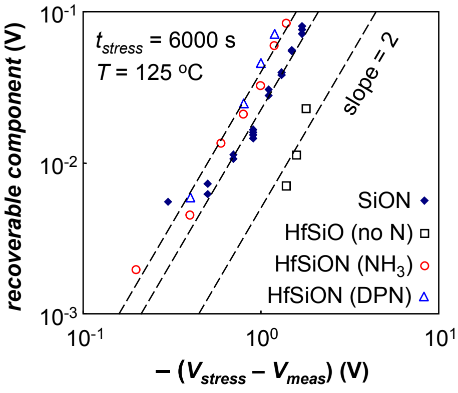

Figure 4. The recoverable component is observed to increase as $(V_{stress}\text{-}V_{meas})^2$. Note that $V_{meas} \approx V_{th}$ in our eMSM measurements.

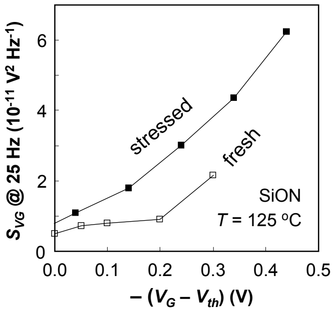

Figure 5. S_{VG} noise increases only ~2× following a NBTI stress resulting in ~ 60 mV threshold voltage shift, corresponding to ~ 6 × 10^{11} cm^{-2} charge density—an order of magnitude increase for a well passivated stack. NBTI stress was applied in two steps, -2 and -2.4V, ~400 s each.

Our NBTI model reported in Ref. [5], designed with the emphasis on capturing the wide temporal distribution of relaxing defects readily reproduces the 1/f noise spectra (Figure 6). The same figure also documents the weak T dependence of S_{VG} at low V_G, observed in Figure 3.

The correlation between S_{VG} and the relaxation component is also strong when comparing nitrided and non-nitrided stacks. As shown in Figure 2, the S_{VG} noise increases approximately tenfold in the nitrided stacks. Coincidentally, the recoverable component increases by the same factor in the nitrided stacks, as shown in Ref. 3. Conversely, we typically see that during stress the recoverable component is increasing only weakly [2], as is also documented by the very low power-law exponents reported by others [12]. This seems consistent with the relatively small increase in S_{VG} [9] after stress that by ΔV_{th} consideration results in more than one decade increase in the total defect density (see Figure 5).

The most intriguing correlation is the apparent quadratic voltage dependence of the recoverable component (Figure 4) [2] and the noise spectra (Figure 2b). The $(V_G\text{-}V_{th})^2$ dependence of S_{VG} has been previously ascribed to channel carrier scattering [13]. In our NBTI model [5] the $(V_{stress}\text{-}V_{th})^2$ dependence of the recoverable component is explained by multiphonon-field-assisted tunneling of holes into defect precursors in the oxide [14]. This allows the model to reproduce the superlinear voltage dependence of S_{VG}.

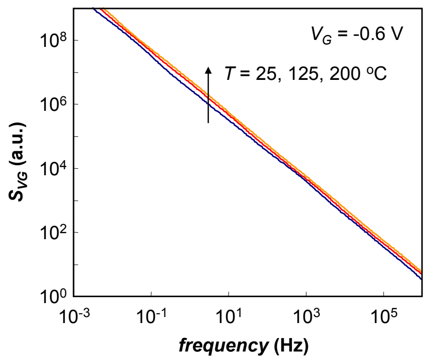

Figure 6. 1/f noise spectra obtained from the equations of our NBTI model [5], corroborating direct correspondence of both phenomena. Also note weak T dependence at low V_G.

All the above arguments are a strong indication of a possible link between NBTI and 1/f noise. Irrespective of the existence of a common physical mechanism, we invoke the *phenomenological* similarities in the last subsection.

B. *NBTI relaxation in very small pFETs*

In small devices, noise typically manifests itself as random telegraph signal. Similarly, the states with widely distributed relaxation times behind NBTI can be readily visualized in small-area pFETs. Discrete NBTI relaxation ΔV_{th} steps corresponding to individual discharging events are clearly apparent in the relaxation transient in Figure 7. The height of the steps varies significantly due to random spatial distribution in the channel plane [15, 16] and cannot be simply ascribed to defect depth in the oxide. By counting individual steps, the average step height is determined to be about 0.6 mV per q, about 3× the value inferred from the simple q/C_{ox} assumption. The factor of 3× is consistent with Ref. [17].

It is moreover apparent from Figure 7 that the down-steps, responsible for the overall relaxation, are *distributed over all measured decades*. This directly confirms our assumption made previously on large pFETs. The same trend is apparent in Figure 8 showing the relaxation transients of 11 small devices. Again, counting individual steps allows us to construct the secondary y-axis in Figure 8.

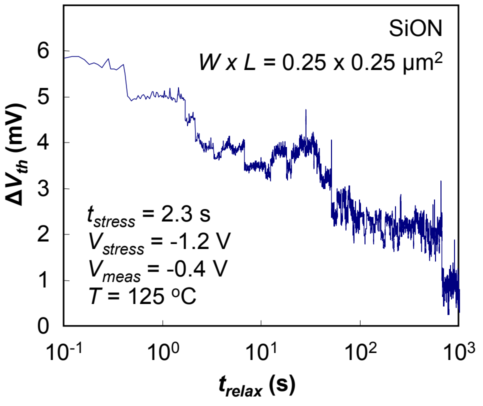

Figure 7. Individual down-steps due to deactivation of discrete defects are clearly visible in every decade of the relaxation transient taken on a small pFET, resulting in ~log(t_{relax}) dependence. The average height of a down-step is ~0.6 mV.

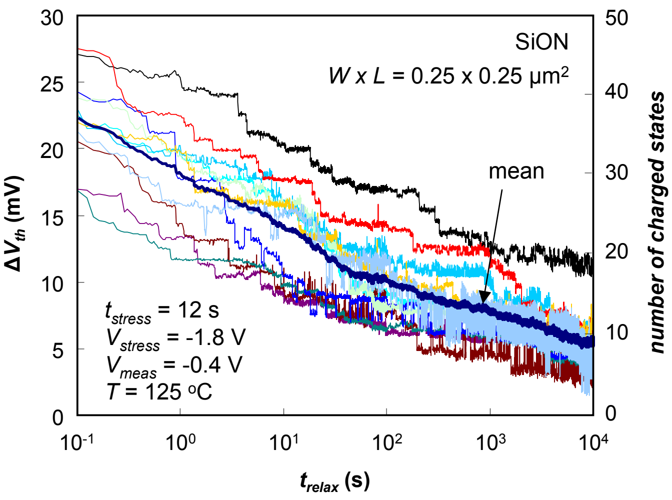

Figure 8. Long relaxation transients taken on 11 different small pFETs. Individual transitions are clearly visible. ΔV_{th} converted to number of charges n (RHS axis) using 0.6 mV/q. The device-to-device spread in ΔV_{th} remains approx. constant with increasing t_{relax}.

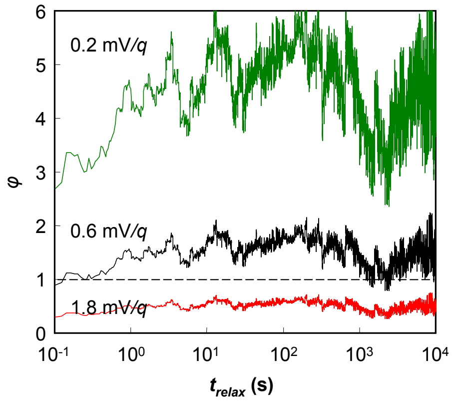

Figure 9. Normalized variance φ = var[$n(t_{relax})$]/<$n(t_{relax})$> with $n(t_{relax})$ from Figure 8 is close to unity (within the limited sample of 11 devices) for 0.6 mV/step, independently confirming this conversion factor. 3× larger and smaller factors are shown for comparison.

While the *mean* of the 11 transients behaves as ΔV_{th} of a large device (e.g. Figure 1a), the device-to-device spread is not decreasing with increasing t_{relax}. Normalized device-to-device variance φ of the number of defect states n [17] (Figure 9) is approximately constant, revealing Poisson statistics [i.e., var(n) = <n>] of the number of defect states. $\varphi \approx 1$ is achieved with the 0.6 mV/q conversion. This conversion factor is thus *independently* confirmed by statistical means [18].

C. NBTI from the perspective of defect states with widely distributed time scales

As already implied above, the defects created during NBTI stress do not have a single, but rather widely varying time constants. Below we show how to visualize this property and within this framework we briefly discuss how the fraction of active defects is affected by the different applications of NBTI stress. We explain on the example of a very small device how the distribution of the defect times should be considered.

We start by noting that in either NBTI relaxation or 1/f noise measurements, no maximum or minimum times are typically observed. For the sake of simplicity we therefore assume here that the time constants are log-uniformly distributed from times much shorter than the switching time of a pFET to very long, corresponding to lifetime of a CMOS application. To facilitate semi-quantitative simulations, defect states are represented by "RC" elements (Figure 10 [2]) with the total pFET ΔV_{th} being proportional to the sum of voltages ("occupancies") on all capacitors. To facilitate our explanation, we first consider that all RC elements have the same weight and can be partially occupied, which would emulate the behavior of a large-area device.

Figure 11a visualizes the log-uniformly distributed "states" with different time constants sequentially charging as the consequence of constant DC stress, a.k.a. the "on-the-fly" (OTF) NBTI measurement. As expected, the fastest states charge first, with slower states becoming occupied as the stress time increases. Upon the removal of the stress (Figure 11b), the fastest states are quickly discharged, illustrating why we observe only a fraction of all states during eMSM recovery sampling (e.g. Figures 7 and 8).

In the case of a digital alternating ("AC") waveform, some states will be only partially represented in ΔV_{th} [19]. This is illustrated in Figure 12 for the varying Duty Factor of the AC stress waveform. States with very short time constants will be again instantly occupied upon the application of stress (cf. Figure 11a). Conversely, states with time constants comparable to the reciprocal frequency of the applied signal will respond and will be (on average) only partially occupied.

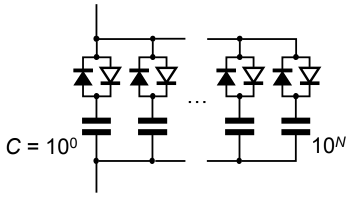

Figure 10. Equivalent circuit with exponentially increasing capacitances used to emulate defect states with widely distributed time scales [2]. The sum of voltages on capacitors is proportional to pFET ΔV_{th}. Note also that the time constants are voltage dependent (e.g., 0.1 s stress results in 10^5 s relaxation, Figure 1a), represented by asymmetric diodes. This crucial property of NBTI is discussed in Ref. [5].

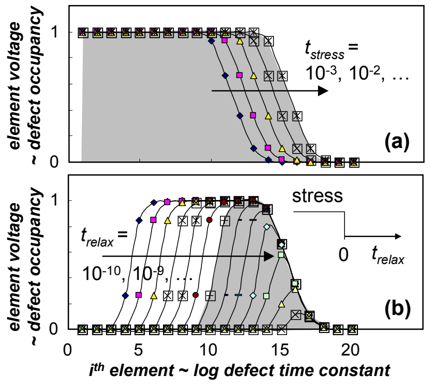

Figure 11. (a) Voltage on capacitors, or occupation of defect states during DC stressing. Grey region represents charged states contributing to ΔV_{th} during this OTF NBTI measurement. (b) Upon recovery, the fastest states discharge immediately. Grey region represents remaining states visible to ΔV_{th} during standard eMSM measurement.

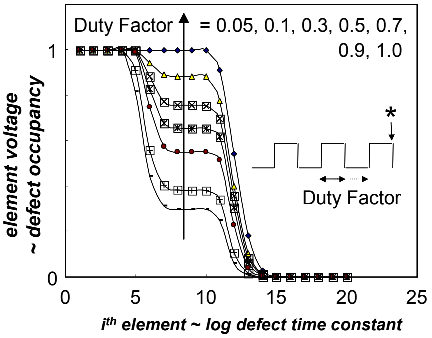

Figure 12. Occupation of states during AC stressing, illustrated in the inset (observed at the end of the "on" phase, marked by *). States with time constants ~ 1/frequency are only partially filled. The Duty Factor is defined as the ratio between the "on" (i.e., the stress) phase and the waveform period.

In a digital inverter, the pFET V_{th} shift influences the delay only when the pFET is turning on [20]. This case is visualized in Figure 13 for a 50% Duty Factor AC input signal. As can be seen in this example, only a subset of all states will be affecting this inverter transition. Comparison with Figure 11 illustrates the discrepancy with the fraction of charged states observed in both most common NBTI tests. In particular, the OTF test substantially overestimates the number of charged defects, i.e., the ΔV_{th}, over the real-world case.

On the other hand, in some other applications, such as the SRAM, some pFETs can be *continuously* on, and hence stressed, for extensive periods of time. As we have shown above, the number of defects in such minimum-size pFETs will be governed by the Poisson distribution. To calculate the number of charged defects for each pFET instance at a given stress time, the widely distributed time scales of the defects need to be considered as well. The result of such calculation in Figure 14 illustrates that if a particular pFET exists in the population with a large number of defects *and* the time scales of those defects are cumulated at shorter times (see "device 1"), the premature failure of the application could occur.

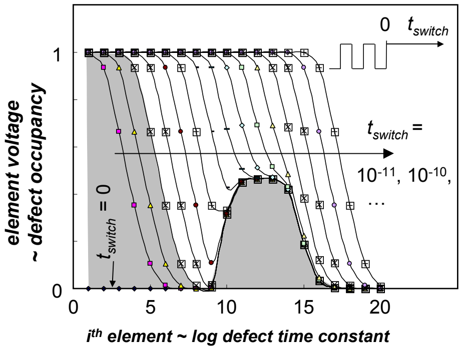

Figure 13. Occupation of states following pFET V_G switching from 0 to V_{DD} (see inset), corresponding to digital inverter input switching from H to L. Only grey region states contribute to ΔV_{th} (cf. Figures 11 and 12) and affect the delay of the digital inverter [20].

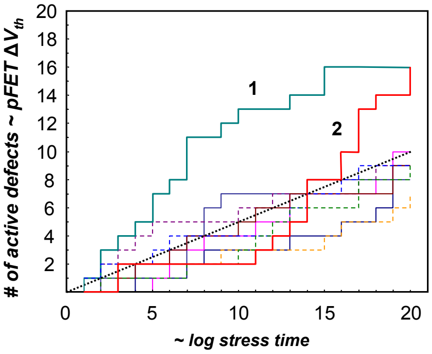

Figure 14. A Monte Carlo calculation of 10 small pFETs with Poisson-distributed number of defects (<n> = 10) and with widely distributed time constants. In this simplified calculation, the latter is done by randomly selecting one RC element (Figure 10) for each defect present in a particular pFET instance. Devices 1 and 2 have the same number of defects but device 1 has defect time scales cumulated at shorter times. The dotted line represents the expected *average* shift in large devices.

IV. CONCLUSIONS

Broad similarity between NBTI relaxation and 1/f noise was observed. Primarily, this correspondence is due to both phenomena being caused by states with widely distributed time scales. Similarly to random telegraph signal, individual transitions in NBTI relaxation in small pFETs were observed and their basic temporal and device-to-device properties were discussed. A distributed "RC" circuit was used to semi-quantitatively visualize active defects during the different applications of NBTI stress. Finally, we showed how the wide distribution of defect times should be considered in addition to defect number variation when estimating worst case NBTI reliability of small devices.

ACKNOWLEDGMENTS

This work was carried out as part of IMEC's Industrial Affiliation Program funded by IMEC's core partners and has been partially supported by the Spanish MICINN (BES-2005-10870).

REFERENCES

[1] E. Milotti, "1/f noise: a pedagogical review", arXiv:physics/0204033v1.

[2] B. Kaczer, T. Grasser, Ph. J. Rousse, J. Martin-Martinez, R. O'Connor, B. J. O'Sullivan, G. Groeseneken, "Ubiquitous Relaxation in BTI stressing—New Evaluation and Insights", *Proc. Int. Reliab. Phys. Symp.*, p. 20, 2008.

[3] M. Aoulaiche, B. Kaczer, Ph. J. Roussel, and R. O'Connor, M. Houssa, S. De Gendt, H. E. Maes, and G. Groeseneken, "Impact of nitridation on recoverable and permanent negative bias temperature instability degradation in high-k/metal-gate p-type metal oxide semiconductor field effect transistors", *J. Vac. Sci. Technol. B* **27**, p. 463, 2009.

[4] T. Grasser, B. Kaczer, P. Hehenberger, W. Gös, R. O'Connor, H. Reisinger, W. Gustin, and C. Schlünder, "Simultaneous Extraction of Recoverable and Permanent Components Contributing to Bias-Temperature Instability," in *IEDM Tech. Digest*, p. 801, 2007.

[5] T. Grasser, B. Kaczer, W. Goes, Th. Aichinger, Ph. Hehenberger, and M. Nelhiebel, "A Two-Stage Model for Negative Bias Temperature Instability", *Proc. Int. Reliab. Phys. Symp.*, 2009.

[6] H. Reisinger, O. Blank, W. Heinrigs, A. Mühlhoff, W. Gustin, and C. Schlünder, "Analysis of NBTI Degradation- and Recovery-Behavior

Based on Ultra Fast V_T-Measurements," in *Proc. Int. Reliab. Phys. Symp.*, p. 448, 2006.

[7] A. Kerber, K. Maitra, A. Majumdar, M. Hargrove, R. J. Carter, and E. A. Cartier, "Characterization of Fast Relaxation During BTI Stress in Conventional and Advanced CMOS Devices With HfO_2/TiN Gate Stacks", *IEEE T. Electron Dev.* **55**, p. 3175, 2008.

[8] R. Jayaraman and C. G. Sodini, "1/f Noise Interpretation of the Effect of Gate Oxide Nitridation and Reoxidation on Dielectric Traps", *IEEE T. Electron Dev.* **37**, p. 305, 1990.

[9] G. Kapila, N. Goyal, V. D. Maheta, C. Olsen, K. Ahmed, and S. Mahapatra, "A Comprehensive Study of Flicker Noise in Plasma Nitrided SiON p-MOSFETs: Process Dependence of Pre-Existing and NBTI Stress Generated Trap Distribution Profiles", *IEDM Tech. Digest*, p. 103, 2008.

[10] D. M. Fleetwood, H. D. Xiong, Z.-Y. Lu, C. J. Nicklaw, J. A. Felix, R. D. Schrimpf, and S. T. Pantelides, "Unified Model of Hole Trapping, 1/f Noise, and Thermally Stimulated Current in MOS Devices", *IEEE T. Nucl. Sci.* **49**, p. 2674, 2002.

[11] B. Moyzhes and T. H. Geballe, S. Jeong, D. Gitlin, and J. Karp, "Current through SiO_2 gate oxide and its low frequency fluctuations: Trapping on charged dangling bonds with negative Hubbard U", *J. Appl. Phys.* **97**, p. 074104, 2005.

[12] C. Shen, M.-F. Li, C. E. Foo, T. Yang, D. M. Huang, A. Yap, G. S. Samudra, and Y.-C. Yeo, "Characterization and Physical Origin of Fast V_{th} Transient in NBTI of pMOSFETs with SiON Dielectric," in *IEDM Tech. Digest*, p. 333, 2006.

[13] G. Ghibaudo O. Roux, Ch. Nguyen-Duc, F. Balestra, and J. Brini, "Improved Analysis of Low Frequency Noise in Field-Effect MOS Transistors", *Phys. Stat. Sol. (a)* **124**, p. 571, 1991.

[14] S. D. Ganichev, W. Prettl, and I. N. Yassievich, "Deep Impurity-Center Ionization by Far-Infrared Radiation," *Phys. Solid State* **39**, p. 1703, 1997.

[15] A. Asenov, "Random dopant induced threshold voltage lowering and fluctuations in sub-0.1 μm MOSFET's: A 3-D 'atomistic' simulation study", *IEEE T. Electron Dev.* **45**, p. 2505, 1998.

[16] M.-J. Chen, C.-C. Lee, and M.-P. Lu, "Probing a nonuniform two-dimensional electron gas with random telegraph signals", *J. Appl. Phys.* **103**, p. 034511, 2008.

[17] S. E. Rauch, "Review and Reexamination of Reliability Effects Related to NBTI-Induced Statistical Variations", *IEEE T. Device Mat. Reliab.* **7**, p. 524, 2007.

[18] D. Ielmini, private communication.

[19] A. P. van der Wel, E. A. M. Klumperink, S. L. J Gierkink, R. F. Wassenaar, and H. Wallinga, "MOSFET 1/f Noise Measurement Under Switched Bias Conditions", *IEEE Electron Dev. Lett.* **21**, p. 43, 2000.

[20] S.-M. Kang and Y. Leblebici, "CMOS Digital Integrated Circuits: Analysis and Design", 2nd international edition, McGraw-Hill, p. 210, 1999.